ISING MODEL FORMULATION OF OUTLIER REJECTION, WITH APPLICATION IN WIFI BASED POSITIONING

Muhammed Tahsin Rahman* *Shuo Han** *Navid Tadayon** *Shahrokh Valaee**

* University of Toronto
Electrical and Computer Engineering
ON, CA, M5S 2E4

ABSTRACT

Multipath interference causes the antenna array of an anchor to estimate several angles of arrival (AoA) for a single user. The resulting ambiguity regarding the line of sight (LoS) component can lead to severe errors in location estimation. This work formulates the problem within an outlier rejection framework: a set of candidate locations are computed by considering all AoAs at all anchors; with the observation that LoS AoA vary less than non-LoS AoA, over several time instances an inlier set can be found that clusters around the true user location. This work then derives an Ising model representation for finding the inlier set and solves the NP-hard problem using the Digital Annealer (DA). Simulations show that this approach improves median localization accuracy by 48.5% when compared to the state-of-the-art in localization methods.

***Index Terms*—** Localization, CSI, Digital Annealer, Ising Model, Outlier Rejection

1. INTRODUCTION

The widespread availability of WiFi technology has played a major role in shifting gears towards a more robust, accurate, ubiquitous, and cost-effective positioning solution. Several pilot projects [1, 2, 3] have shown that, through advanced signal processing, WiFi signals based on MIMO-OFDM technology can be used to localize mobile users with unprecedented accuracy when line-of-sight (LoS) exists and the multipath environment is not too dispersive. It is in a shadowed and highly reflective environment that we develop an approach to localize a user.

1.1. Relation to Prior Work

With the advent of a toolkit [4] that enables channel state information (CSI) to be recorded from commodity 802.11n network interface cards, several works have emerged that leverage angle of arrival (AoA) and time of flight (ToF) estimation techniques to localize a user using the exposed CSI data. However, a major source of error arises by the fact that such estimation algorithms lead to detecting several reflections of the same incoming signal, a phenomenon caused by multipath interference.

A whole body of literature aims to tackle errors in LoS detection. For instance, [5, 6] use the fundamental observation that the LoS signal must arrive earlier than any reflections. As such, mean excess delay and kurtosis statistics are used to study the signal delay. A similar approach is presented in [7], where the statistics of an incoming signal are computed and compared to statistics of LoS signals; anchors are then detected as being LoS or NLoS. Within a WiFi-OFDM framework, [1] rely on a compressive sensing approach to identify incoming signal paths and then choose the path that has shortest arrival time. However, we frequently encounter the situation where one or more anchors are heavily shadowed (and we are unaware) or the situation where the environment is too scattering / reflective that LoS and non-LoS rays are comparable in power and in arrival times. To overcome this challenge, another method for LoS identification is [8], where a user's motion is used to distinguish the stationary LoS signal from the highly fluctuating non-LoS signals. In this vein, [9] proposes a neural network approach to identify LoS when a user is stationary and K-means clustering when the user is mobile. Despite advances in LoS detection, there is a common underlying paradigm: the localization and LoS detection stages are taken to be separate.

In one of the first works that achieves decimeter-level localization accuracy on a practical CSI-based WiFi testbed, the authors have considered estimating location without first performing LoS detection [3]. Our work proceeds in a similar fashion (and indeed compares results to their algorithm), while taking advantage of the fact that LoS signals have different statistical properties as compared to NLoS signals.

1.2. Contributions

This paper tackles the localization problem through an outlier rejection approach. Instead of ruling out all AoAs but one

The authors would like to thank Fujitsu Laboratories Ltd. and Fujitsu Consulting (Canada) Inc. for providing access to Digital Annealer at the University of Toronto.

(the one deemed to be due to LoS), here we keep all AoAs estimated by all anchors for several consecutive packets and form the set of all the candidate locations. Leveraging the spatio-temporal correlations between candidate locations, we decide on an inlier set and recover the true location.

Furthermore, to decide on an inlier set we develop an outlier rejection algorithm based on the Ising model, a combinatorial formulation originating in statistical physics. Solving this NP-hard problem using the Digital Annealer (DA), our results show that large gains in performance are obtainable in both low and high SNR regimes when compared to recent indoor positioning systems.

In developing our methodology, section 2 formalizes the problem as an outlier rejection one. Next, section 3 formulates outlier rejection as an Ising model and introduces the DA and M-sample consensus (MSAC) based outlier rejection [10]. Section 4 presents simulation results and performance comparisons. Finally, section 5 concludes.

2. PROBLEM FORMULATION

At discrete time instant (s) consider a receiver at position $\boldsymbol{x}^{(s)} \in \mathbb{R}^2$ that communicates with A anchors. Given that each anchor, $a \in \{1, 2, ..., A\}$, estimates $\hat{\boldsymbol{\theta}}_a^{(s)}$ angles of arrival (AoA), such that the number of AoA estimates $\left|\hat{\boldsymbol{\theta}}_a^{(s)}\right| = M_a^{(s)}$, we wish to find the position $\boldsymbol{x}^{(s)}$ of the receiver.

Using $\hat{\boldsymbol{\theta}}_a^{(s)}$ and knowledge of the anchor position and orientation, construct a set of rays $\vec{\boldsymbol{R}}_a^{(s)}$ in a consistent global coordinate system, with each $\vec{R}_{a,i}^{(s)} \in \vec{\boldsymbol{R}}_a^{(s)}$ having origin at the anchor location and extending in the direction of the rotated AoA $\hat{\theta}_{a,i}^{(s)} \in \hat{\boldsymbol{\theta}}_a^{(s)}, \forall i \in \left\{1, 2, ..., M_a^{(s)}\right\}$.

For a single pair $\vec{R}_{a_1,i}^{(s)}, \vec{R}_{a_2,j}^{(s)}$, where $a_1, a_2 \in \{1, 2, ..., A\}$ and $a_1 \neq a_2$ we compute a candidate location $\dot{\boldsymbol{x}}_{a_1 i, a_2 j}$ by finding the coordinates of the intersection of the two rays. Repeating the same for every pair of rays at every pair of anchors, results in a set of candidate locations given by

$$\dot{\boldsymbol{X}}^{(s)} = \bigcup_{a_1 < a_2} \bigcup_{i,j} \dot{\boldsymbol{x}}_{a_1 i, a_2 j}^{(s)}, \tag{1}$$

$\forall\, a_1, a_2 \in \{1, 2, ..., A\}$, $\forall\, i \in \{1, 2, ..., M_{a_1}\}$, $\forall\, j \in \{1, 2, ..., M_{a_2}\}$, and $\dot{\boldsymbol{X}} \in \mathbb{R}^{K_{tot}\,\mathrm{x}\,2}$ with K_{tot} representing the total number of candidate locations. As observed by several works mentioned in section 1.1, the AoA from the line of sight (LoS) component exhibits less variation than that of reflected components. This observation can be leveraged by considering several time instances simultaneously and constructing the set $\dot{\boldsymbol{X}}^{(1 \cdots S)} = \bigcup_{s=1}^{S} \dot{\boldsymbol{X}}^{(s)}$. Furthermore, observe that candidate locations will tend to cluster around the true user location given sufficient time instances S. The problem is now reduced to finding an inlier set $\tilde{\boldsymbol{X}} \subseteq \dot{\boldsymbol{X}}^{(1 \cdots S)}$ whose elements are most similar. Note that if only the LoS AoA is estimated at each time instant and each anchor, then $\tilde{\boldsymbol{X}} = \dot{\boldsymbol{X}}^{(1 \cdots S)}$. Finally, the user location can be found as

$$\hat{\boldsymbol{x}} = \frac{1}{K_{in}} \boldsymbol{1}^\top \tilde{\boldsymbol{X}}, \tag{2}$$

where the size of the inlier set $K_{in} = \left|\tilde{\boldsymbol{X}}\right|$ and $\boldsymbol{1}$ is the all-ones vector of size K_{in}. Fig. 1a shows the rays traced out by four anchors and the corresponding intersection points $\dot{\boldsymbol{X}}^{(1)}$. Fig. 1b plots all the candidate points $\dot{\boldsymbol{X}}^{(1 \cdots 10)}$. After computing these points, two methods of finding $\tilde{\boldsymbol{X}}$ are presented in the following section.

3. METHODOLOGY

We first generalize (2) using the entire candidate set as

$$\hat{\boldsymbol{x}} = \frac{1}{\boldsymbol{y}^\top \boldsymbol{y}} \boldsymbol{y}^\top \dot{\boldsymbol{X}}, \tag{3}$$

where $\boldsymbol{y} \in \{0, 1\}^{K_{tot}}$ and the superscript on $\dot{\boldsymbol{X}}^{(1 \cdots S)}$ has been dropped to ease notation. The vector $\boldsymbol{y}$ is a binary selection vector such that $y_i = 1$ means that $\dot{\boldsymbol{x}}_i \in \tilde{\boldsymbol{X}}$ and $y_i = 0$ means that $\dot{\boldsymbol{x}}_i \in \tilde{\boldsymbol{X}}^{\mathsf{c}}$.

3.1. Ising Model for Outlier Rejection

The Ising model is a quadratic form representation of a system consisting of binary states that are bidirectionally connected. It is characterized by the Ising energy function

$$E(\boldsymbol{y}; \boldsymbol{W}, \boldsymbol{b}) = -\sum_i \sum_j W_{ij} y_i y_j - \sum_i b_i y_i, \tag{4}$$

where the state $y_i \in \{0, 1\}$ and the parameters $W_{i,j}, b_i \in \mathbb{R}\, \forall\, i, j$. Finding the minimum Ising energy is a famously NP hard problem. However, there exist solvers (for instance, [11] uses GPU parallel processing and [12] uses physical magnetic tunnel junctions), of which the DA is a promising one that will be introduced in section 3.2. Our goal is to find the weights $\boldsymbol{W}$ and biases $\boldsymbol{b}$ so that we can solve for $\boldsymbol{y}$ by minimizing the Ising energy.

Firstly, the error between the estimate $\hat{\boldsymbol{x}}$ in (3) and a single candidate location $\dot{\boldsymbol{x}}_i$ is

$$\begin{aligned} \hat{d}_i(\hat{\boldsymbol{x}}, \dot{\boldsymbol{x}}_i) &= |\hat{\boldsymbol{x}} - \dot{\boldsymbol{x}}_i|_2^2 \\ &= \left(\frac{\boldsymbol{y}^\top \dot{\boldsymbol{X}}}{\boldsymbol{y}^\top \boldsymbol{y}} - \dot{\boldsymbol{x}}_i\right)^\top \left(\frac{\boldsymbol{y}^\top \dot{\boldsymbol{X}}}{\boldsymbol{y}^\top \boldsymbol{y}} - \dot{\boldsymbol{x}}_i\right) \\ &= \frac{1}{(\boldsymbol{y}^\top \boldsymbol{y})^2} \left(\boldsymbol{y}^\top \dot{\boldsymbol{X}} \dot{\boldsymbol{X}}^\top \boldsymbol{y}\right) \\ &\qquad - \frac{2}{\boldsymbol{y}^\top \boldsymbol{y}} \boldsymbol{y}^\top \dot{\boldsymbol{X}} \dot{\boldsymbol{x}}_i + \dot{\boldsymbol{x}}_i^\top \dot{\boldsymbol{x}}_i. \end{aligned} \tag{5}$$

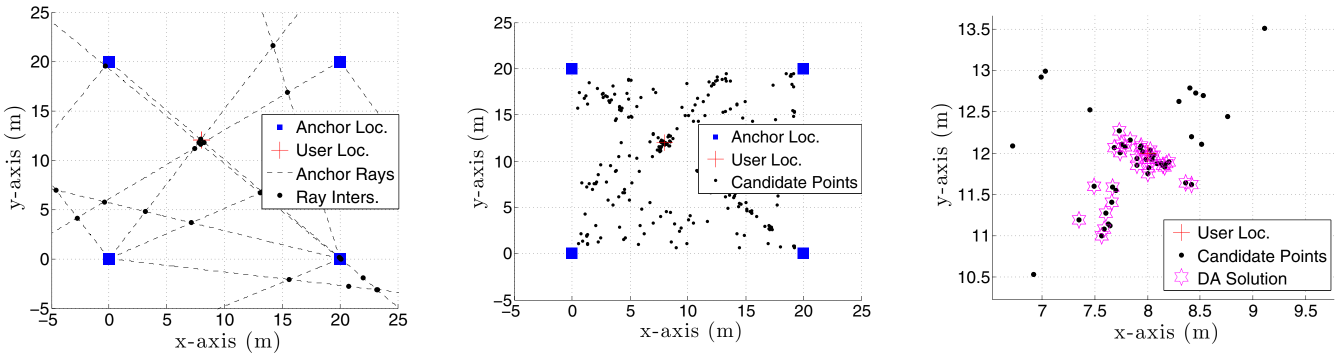

(a) AoA estimates and ray intersections (b) Candidate locations for $S = 10$ (c) DA solution

Fig. 1: (a) shows four anchors, their respective rays, and the ray intersections. In (b) the pairwise intersections are shown for $S = 10$ within a region of interest 20mx20m. (c) zooms in to the user location, showing the inlier set selected using the DA

Stacking the errors for $\dot{\boldsymbol{x}}_i \, \forall \, i$ gives

$$\hat{\boldsymbol{d}}(\hat{\boldsymbol{x}}, \dot{\boldsymbol{X}}) = \frac{1}{\left(\boldsymbol{y}^\top \boldsymbol{y}\right)^2} \left(\boldsymbol{y}^\top \dot{\boldsymbol{X}} \dot{\boldsymbol{X}}^\top \boldsymbol{y}\right) \boldsymbol{1} - \frac{2}{\boldsymbol{y}^\top \boldsymbol{y}} \dot{\boldsymbol{X}} \dot{\boldsymbol{X}}^\top \boldsymbol{y} + \operatorname{diag}\left(\dot{\boldsymbol{X}} \dot{\boldsymbol{X}}^\top\right).$$

We wish to find $\boldsymbol{y}$ to minimize the total error within the inlier set,

$$\begin{aligned} \hat{\boldsymbol{y}} &= \arg\min_{\boldsymbol{y}} \boldsymbol{y}^\top \hat{\boldsymbol{d}}(\hat{\boldsymbol{x}}, \dot{\boldsymbol{X}}) \\ &= \arg\min_{\boldsymbol{y}} -\frac{1}{(\boldsymbol{y}^\top \boldsymbol{y})} \left(\boldsymbol{y}^\top \dot{\boldsymbol{X}} \dot{\boldsymbol{X}}^\top \boldsymbol{y}\right) + \boldsymbol{y}^\top \operatorname{diag}\left(\dot{\boldsymbol{X}} \dot{\boldsymbol{X}}^\top\right). \end{aligned}$$

The $\frac{1}{(\boldsymbol{y}^\top \boldsymbol{y})}$ term prevents the conversion to a quadratic form. Hence, let $\boldsymbol{y}^\top \boldsymbol{y} = \sum_i y_i = K_{in}$ be a fixed parameter. It should be noted that if we were to assume every anchor estimates a single AoA at time s, then for S instances $K_{tot} = S \cdot \frac{A(A-1)}{2}$. Practically not all anchors will estimate the true AoA, and even if they did there would be instances where the error was large; therefore, in our implementation we chose $K_{in} = S \cdot \frac{A(A-1)}{4}$.

Incorporating this constraint as $\lambda \left(K_{in} - \boldsymbol{1}^\top \boldsymbol{y}\right)^2$ for some large λ yields

$$\begin{aligned} \hat{\boldsymbol{y}} &= \arg\min_{\boldsymbol{y}} -\frac{1}{K_{in}} \boldsymbol{y}^\top \dot{\boldsymbol{X}} \dot{\boldsymbol{X}}^\top \boldsymbol{y} \\ &\qquad + \boldsymbol{y}^\top \operatorname{diag}\left(\dot{\boldsymbol{X}} \dot{\boldsymbol{X}}^\top\right) + \lambda \left(K_{in} - \boldsymbol{1}^\top \boldsymbol{y}\right)^2 \\ &= \arg\min_{\boldsymbol{y}} -\boldsymbol{y}^\top \left(\frac{\dot{\boldsymbol{X}} \dot{\boldsymbol{X}}^\top}{K_{in}} - \lambda\right) \boldsymbol{y} \\ &\qquad - \boldsymbol{y} \top \left(-\operatorname{diag}\left(\dot{\boldsymbol{X}} \dot{\boldsymbol{X}}^\top\right) + 2\lambda K_{in} \boldsymbol{1}\right). \end{aligned}$$

If we let $\tilde{\boldsymbol{W}} = \frac{\dot{\boldsymbol{X}} \dot{\boldsymbol{X}}^\top}{K_{in}} - \lambda$ and $\tilde{\boldsymbol{b}} = -\operatorname{diag}\left(\dot{\boldsymbol{X}} \dot{\boldsymbol{X}}^\top\right) + 2\lambda K_{in} \boldsymbol{1}$, we have

$$\hat{\boldsymbol{y}} = \arg\min_{\boldsymbol{y}} E(\boldsymbol{y}; \tilde{\boldsymbol{W}}, \tilde{\boldsymbol{b}}), \tag{6}$$

which is in the same form as (4). Having solved for $\hat{\boldsymbol{y}}$, the user location is given by (3).

3.2. Digital Annealer

The DA [13] is a technology to solve large-scale combinatorial optimization problems by an annealed Markov chain Monte Carlo (MCMC) search. The Ising energy, shown previously in (4), can be solved for 1024 fully connected binary states. The weight between any two binary variables is represented by 16-bits.

At each MCMC iteration, the DA calculates the change in the Ising energy function for each of the 1024 bit flips in parallel. The acceptance probability of a bit flip is computed based on the Metropolis criterion [14]. This process is repeated for a large number of iterations, while simultaneously annealing the system temperature. With regards to speed-up, the DA has demonstrated approximately two orders of magnitude improvement than state-of-the-art simulated annealing (SA) for fully-connected spin-glass problems [15].

3.3. MSAC Outlier Rejection

In MSAC based outlier rejection [10], a minimum number of points needed to instantiate a solution are picked uniformly at random. In our case, this is a single point with index i. Next, the distance between this selected point and a candidate location is computed and thresholded based on some preset value t, expressed as

$$\dot{d}_i(\dot{\boldsymbol{x}}_i, \dot{\boldsymbol{x}}_j) = \min\left(|\dot{\boldsymbol{x}}_i - \dot{\boldsymbol{x}}_j|_2^2, t\right) \quad i \neq j. \tag{7}$$

Note the subtle difference between (7) and (5). Both compute the distance between the estimated location and other candidate locations. However, (7) is a simplification of (5) in that it only considers a single candidate location as the estimate at a given sampling iteration. The Ising model formulation, on the other hand, considers a set of candidate locations as the estimate at each sampling iteration.

For the MSAC approach, the number of random samples that should be considered are based on the desired probability of success of the algorithm [16],

$$Pr = 1 - (1 - (1 - \epsilon)^p)^m,$$

where ϵ is the proportion of outliers, p is the minimum number of points to instantiate a solution, and m is the number of samples considered.The optimum candidate point index is found as

$$k = \arg\min_i \sum_{j=1, i \neq j}^{K_{tot}} \dot{d}_i(\dot{\boldsymbol{x}}_i, \dot{\boldsymbol{x}}_j)$$

$$i \overset{\overset{m}{\text{i.i.d}}}{\sim} \mathcal{U}\left\{1, 2, ..., K_{tot}\right\}.$$

The binary selection vector is now found as

$$\hat{y}_j = \mathbb{1}\left[|\dot{\boldsymbol{x}}_k - \dot{\boldsymbol{x}}_j|_2^2 < t\right] \quad \forall j \in \{1, 2, ..., K_{tot}\}, \qquad (8)$$

where $\mathbb{1}\left[\cdot\right]$ is the indicator function returning 1 if the argument is true and 0 otherwise. Using $\hat{\boldsymbol{y}}$, the user location is given by (3).

4. RESULTS AND DISCUSSION

We utilize the Winner Phase II (WIM2) channel model [17] to simulate CSI data given a layout of anchors and user locations. The layout considered is the same as in Fig. 1a, with signal to noise ratio of 0dB and 10dB. 16 user locations are simulated covering the entire region of interest. The information inherent within CSI is exploited by several established methods in the literature to estimate AoA, including MUSIC (MU) [18] and matrix pencil (MP) [19], which are both implemented in our simulations.

Several recent works, such as [1] and [3], have proposed using grid search based algorithms over the entire region of interest. For instance, ArrayTrack [3] uses CSI as an input to solve for the pseudo-spectrum at each anchor using MU. For each grid point, ArrayTrack then samples the pseudo-spectra of each anchor at the corresponding AoA that would be observed if a user was at the grid location. The grid point that achieves the maximum sum of sampled pseudo-spectra across all anchors is chosen as the user location. This method is adopted as a baseline in our work since the accuracy of ArrayTrack rivals that of other methods when the size of the antenna array is large, about 8 elements per anchor [2]. Therefore, we fix our anchors with 8 antenna elements each, keeping the ArrayTrack algorithm as a viable option for the baseline.

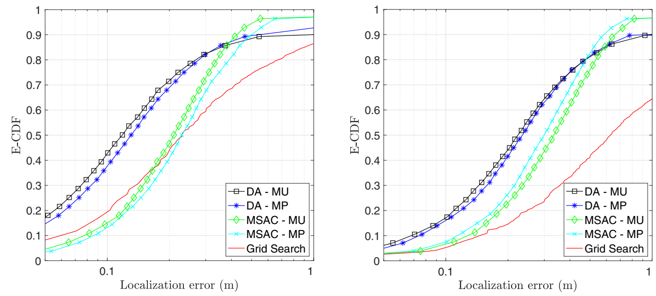

(a) SNR 10dB (b) SNR 0dB

Fig. 2: Plots of the performance across test locations

Fig. 2 plots the empirical cumulative distribution function (ECDF) of the error for five different implementations. The abbreviation DA-MU refers to AoA estimation using MUSIC and location estimation using the Ising model formulation of section 3.1; MSAC uses the formulation of section 3.3; Grid Search refers to our ArrayTrack implementation.

We see from Fig. 2a that the DA based implementation leads to a median accuracy of 0.12m, a 48.5% improvement over grid search (0.23m) and a 43.6% improvement over the MSAC approach (0.21m). Both MSAC and grid search were quite similar. At 0dB SNR, shown in Fig. 2b the DA implementation drops in accuracy to 0.22m; however, grid search drops to 0.62m (65% less than DA) and MSAC drops to 0.30m (25% less than DA). Overall, the outlier rejection algorithms seem more robust to reduced SNR than the grid search. One explanation for this observation is that the pseudo-spectrum of MU becomes wider lobed at lower SNR; sampling the spectra based on the grid points would lead to similar values across larger swaths of the grid, resulting in reduced accuracy. The outlier rejection methods consider only the estimated AoA, known to be unbiased, which leads to greater accuracy.

5. CONCLUSION

The key observation that an estimated AoA from the LoS signal has less variance than estimated AoA from non-LoS signals motivated the formulation of multiple anchor localization in the presence of multipath interference as an outlier rejection problem. This work also developed outlier rejection as a combinatorial optimization problem in the Ising model framework. The DA was used to efficiently solve the NP-hard problem and its performance was compared to MSAC based outlier rejection and a state-of-the-art localization technique.

6. ACKNOWLEDGEMENT

The authors would like to thank Fujitsu Laboratories Ltd. and Fujitsu Consulting (Canada) Inc. for providing access to Digital Annealer at the University of Toronto.

7. REFERENCES

[1] W. Gong and J. Liu, "RoArray: Towards more robust indoor localization using sparse recovery with commodity WiFi," *IEEE Transactions on Mobile Computing*, 2018.

[2] M. Kotaru, K. Joshi, D. Bharadia, and S. Katti, "Spotfi: Decimeter level localization using WiFi," *SIGCOMM Comput. Commun. Rev.*, vol. 45, no. 4, pp. 269–282, Aug. 2015.

[3] J. Xiong and K. Jamieson, "Arraytrack: A fine-grained indoor location system," in *10th USENIX Symposium on Networked Systems Design and Implementation (NSDI 13)*, Lombard, IL, 2013, pp. 71–84, USENIX.

[4] D. Halperin, W. Hu, A. Sheth, and D. Wetherall, "Tool release: Gathering 802.11n traces with channel state information," *SIGCOMM Comput. Commun. Rev.*, vol. 41, no. 1, pp. 53–53, 2011.

[5] L. Mucchi and P. Marcocci, "A new parameter for UWB indoor channel profile identification," *IEEE Transactions on Wireless Communications*, vol. 8, no. 4, pp. 1597–1602, April 2009.

[6] İ. Güvenç, C. Chong, F. Watanabe, and H. Inamura, "NLoS Identification and Weighted Least-squares Localization for UWB Systems Using Multipath Channel Statistics," *Journal on Advances in Signal Processing*, 2007.

[7] Y. Chan, W. Tsui, H. So, and P. Ching, "Time-of-arrival based localization under NLOS conditions," *IEEE Transactions on Vehicular Technology*, vol. 55, no. 1, pp. 17–24, 2006.

[8] Z. Zhou, Z. Yang, C. Wu, L. Shangguan, H. Cai, Y. Liu, and L. M. Ni, "WiFi-based indoor line-of-sight identification," *IEEE Transactions on Wireless Communications*, vol. 14, no. 11, pp. 6125–6136, 2015.

[9] F. Xiao, Z. Guo, H. Zhu, X. Xie, and R. Wang, "AmpN: Real-time LOS/NLOS identification with WiFi," in *2017 IEEE International Conference on Communications (ICC)*, 2017, pp. 1–7.

[10] P. H. S. Torr and A. Zisserman, "MLESAC: A new robust estimator with application to estimating image geometry," *Journal of Computer Vision and Image Understanding*, vol. 78, no. 1, pp. 138 – 156, 2000.

[11] C. Cook, H. Zhao, T. Sato, M. Hiromoto, and S. X. D. Tan, "GPU based parallel Ising computing for combinatorial optimization problems in VLSI physical design," Preprint available at https://arxiv.org/abs/1807.10750, July 2018.

[12] Y. Shim, A. Jaiswal, and K. Roy, "Ising computation based combinatorial optimization using Spin-Hall Effect (SHE) induced stochastic magnetization reversal," *Journal of Applied Physics*, 2018.

[13] S. Matsubara, H. Tamura, M. Takatsu, D. Yoo, B. Vatankhahghadim, H. Yamasaki, T. Miyazawa, S. Tsukamoto, Y. Watanabe, K. Takemoto, and A. Sheikholeslami, "Ising-model optimizer with parallel-trial bit-sieve engine," in *Complex, Intelligent, and Software Intensive Systems*, L. Barolli and O. Terzo, Eds. 2018, pp. 432–438, Springer International Publishing.

[14] N. Metropolis, A. W. Rosenbluth, M. N. Rosenbluth, and A. H. Teller, "Equation of state calculations by fast computing machines," *Journal of Chemical Physics*, vol. 21, pp. 1082–1092, 1953.

[15] M. Aramon, G. Rosenberg, E. Valiante, T. Miyazawa, H. Tamura, and H. G. Katzgraber, "Physics-inspired optimization for quadratic unconstrained problems using a digital annealer," Preprint aAvailable at https://arxiv.org/abs/1806.08815, Aug 2018.

[16] *Robust Regression and Outlier Detection*, John Wiley & Sons, New York, NY, USA, 1987.

[17] L. Hentilä, P. Kyösti, M. Käske, M. Narandzić, and M. Alatossava, "MATLAB implementation of the WINNER Phase II channel model ver1.1," Online, December 2007.

[18] R. Schmidt, "Multiple emitter location and signal parameter estimation," *IEEE Transactions on Antennas and Propagation*, vol. 34, no. 3, pp. 276–280, 1986.

[19] N. Yilmazer, T. K. Sarkar, and M. Salazar-Palma, "DOA estimation using Matrix Pencil and ESPRIT methods using single and multiple snapshots," in *URSI International Symposium on Electromagnetic Theory*, 2010, pp. 215–218.